Journal of Fluorescence, Vol. 15, No. 4, July 2005 (© 2005)
DOI: 10.1007/s10895-005-2826-6

Progress in Lanthanides as Luminescent Probes

I. Hemmilä[1,2] and V. Laitala[1]

Received November 10, 2004; accepted March 1, 2005

Lanthanides have recently found applications in different fields of biomolecular and medical research. Luminescent lanthanide chelates have created interest mainly due to their unique luminescent properties, such as their long Stokes' shift and exceptional decay times allowing efficient temporal discrimination of background interferences in the assays, such as immunoassays. Recently, new organometallic complexes have been developed giving opportunities to novel applications, in heterogeneous and homogeneous immunoassays, DNA hybridization assays, high-throughput screening as well as in imaging. In addition, encapsulating the chelates into suitable matrix in beads enables the use of new members of lanthanides extending the emission wavelength to micrometer range and decays from a few microseconds to milliseconds. As the luminescence is derived from complicated intrachelate energy transfer, it also gives novel opportunities to exploit these levels in different types of energy transfer based applications. This review gives a short overview of recent development of lanthanide chelate-labels and discusses in more details of energy levels and their exploitation in new assay formats.

KEY WORDS: Lanthanide chelates; luminescence; time-resolved fluorometry; fluoroimmunoassays; TR-FIA; TR-FRET; high throughput screening.

INTRODUCTION

Lanthanide chelates, due to their unique luminescence properties, are gaining expanding applications in wide variety of bioanalytical assays, in diagnostic, research, drug discovery, as sensing tools and in imaging. The development of novel, highly luminescent chelates, chelating ligands, and various forms of luminescent lanthanide-based nanobeads has made it possible to construct wide variety of assay technologies enabling not only highly sensitive assays through background discrimination, but also very easy and robust assays suitable for high throughput screening and miniaturization. The unique spectral and temporal properties of lanthanides allow also multi-label assays to monitor several analytes simultaneously or to gather more analytical data from a single sample.

The ligand enhanced lanthanide luminescence is a complicated process involving several energy levels on ligand site and on the excited levels and ground state levels of different ions. Some of the processes are not fully understood, which makes the optimization of chelates complicated. But on the other hand, the complicated nature of energy transfer processes gives new opportunities to develop labels of widely different properties and novel assay technologies to be applied in different applications, e.g. by extending the range of used ions and range of energy transfer processes applied.

In the current review, we concentrate on basic analytical luminescence properties of lanthanide chelates and give a short survey of most recent ligand developments. We collected also an overview of their most recent applications in diagnostics and research. In particular, the applications of various lanthanide chelate probes in assays related to signal transduction and high throughput screening are reviewed.

[1] Perkin Elmer Life and Analytical Sciences, Wallac Oy, P.O. Box 10, FIN-20101, Turku, Finland.
[2] To whom correspondence should be addressed. E-mail: ilkka.hemmila@perkinelmer.com

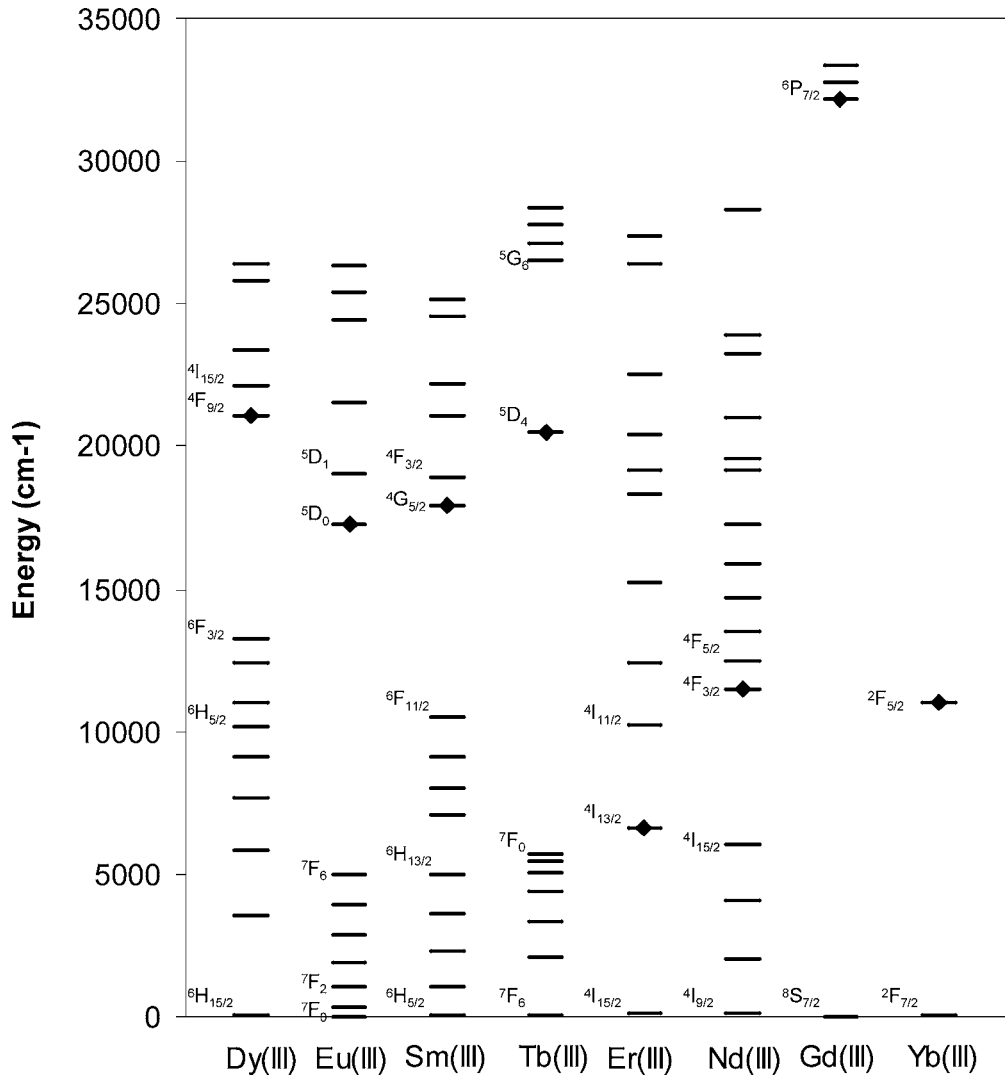

Fig. 1. Energetic levels of various luminescent lanthanides. Black dots relate to the emittive energy level.

LUMINESCENCE PROPERTIES OF LANTHANIDE CHELATES

When chelated with suitable light absorbing ligand, lanthanides express luminescence characterized by ion-specific narrow banded emission lines of exceptionally long decay times. The decays are ranging from upper nanosecond range with ytterbium, neodymium and erbium chelates, to microseconds scale with dysprosium chelates, and up to a few milliseconds with europium and terbium chelates [1,2]. The long decay times were the primary reason to the initial interest to luminescent lanthanide chelates, as they allowed easy and efficient background discrimination by simple and robust gating in the fluorometric analysis [1]. The long decays together with narrow-banded emissions and exceptionally large Stokes' shifts makes lanthanide chelates a versatile group of labels for a wide variety of bioanalytical assays including both heterogeneous and homogeneous assays, assays with multiplexing, and multivariate analysis.

Intrachelate Energy Transfer

Lanthanides express very specific luminescence emissions due to their unfilled 4fn electronic orbital, in which the 4f electrons are well shielded from the environment by the outer core electrons and are minimally involved in bonding. Figure 1 shows a simplified diagram of the relevant energy levels of various luminescent lanthanides [3–6]. The energy flow in the lanthanide

chelate derives from excited singlet level through intersystem crossing to ligand triplet state, and from the ligand triplet state to the emittive levels of the chelated central ion [7]. The trivalent ions in the chelates function both as efficient triplet sensitizers creating rapid and efficient intersystem crossing and as energy acceptors whereby shortening the triplet state lifetimes [8].

Based on a series of ligand triplet state measurements [9,10] and on a theoretical model [11], europium(III) can accept energy by several of its ^5D_j levels provided that they lay below the ligand triplet state, but the major accepting levels seems to be $^5D_1$ and $^5D_2$. Terbium, on the other hand, accepts excited energy directly by its emittive level ($^5D_4$) and does not have other low lying resonance levels involved in the excitation process.

The excitation of lanthanide chelates is mostly restricted to near-UV range, seldom exceeding 350 nm. The maximum excitation is limited by the gap between singlet and triplet state of the ligand [12]. Based on theoretical calculations [13] and in practical measurements [9], europium chelates accept energy only through some of the higher resonance levels and not directly by $^5D_0$, limiting of the possibility of visible excitation. Excitation with a higher wavelength light would be beneficial for instrumental and interference point of view. Near IR emittive lanthanides, erbium, neodymium and ytterbium, due to their lower excited state energies, can be excited with a wider range of antenna moieties.

Excited State Lifetimes

The major transitions in the highly luminescent chelates (e.g. $^5D_0$–$^7F_2$ in Eu(III)) are electric dipole 'forced' and since have relatively long lifetime [14]. The excited state lifetimes of the chelates are regarded to be a function of the natural luminescent lifetime of the central ion and the sum of non-radiative deactivation processes according to equation (1),

$$\tau = \frac{1}{k_r + k_{nr}} \tag{1}$$

where τ is the measured luminescence lifetime, k_r the rate constant for radiative transition of the central ion and k_{nr} is the sum of rate constants for all the non-radiative relaxation processes. Additionally, in luminescent lanthanide chelates the triplet state of the ligand can have a lifetime from few nanoseconds to several microseconds and the intrasystem crossing from ligand to the central ion can have influence on the observed lifetime [8]. The main emittive transitions of some of the lanthanides commonly used in bioanalytical applications are collected in Table I [1,2,15–18].

Table I. The main emittive transitions of some lanthanide metals

Lanthanide (III)	Transition	Emission (nm)	Decay range in solution (μs)
Eu	$^5D_0 \rightarrow {}^7F_0$	580	300–1500
	$^5D_0 \rightarrow {}^7F_2$	613	
	$^5D_0 \rightarrow {}^7F_4$	690	
Tb	$^5D_4 \rightarrow {}^7F_6$	490	100–1500
	$^5D_4 \rightarrow {}^7F_4$	545	
Sm	$^4G_{5/2} \rightarrow {}^6H_{7/2}$	598	20–50
	$^4G_{5/2} \rightarrow {}^6H_{9/2}$	643	
Dy	$^4F_{9/2} \rightarrow {}^6H_{13/2}$	575	1–20
Yb	$^2F_{5/2} \rightarrow {}^2F_{7/2}$	980	0.5–2
Nd	$^4F_{3/2} \rightarrow {}^4F_{13/2}$	880	0.03–1
	$^4F_{3/2} \rightarrow {}^4F_{9/2}$	1065	
Er	$^4I_{13/2} \rightarrow {}^4I_{15/2}$	1522	

In practice, the excited state lifetimes of the chelates are also regarded to be a function of the quantum yield of the central ion q_{Ln}, which is defined by rate constants according to equation (2). The overall quantum yield of the chelate is also affected by the energy transfer efficiency (probability) from the ligand to the central ion.

$$q_{Ln} = \frac{k_r}{k_r + k_{nr}} \tag{2}$$

Chelate-bound, inner sphere water molecules (O−H vibrational overtones) is the most common excited state non-radiative relaxation route with all the luminescent lanthanide chelates (section 'Luminescence Quenching'). Multi-dentate chelates exhibit reduced quenching by water due to better shielding which also results in increased quantum yields and prolonged decay times.

The decay behavior of terbium(III) chelates is more complex. Due to the larger energy gap between the lowest excited level and highest ground state manifold, terbium is not as sensitive to O−H vibrations as the other lanthanides. On the other hand, due to the direct energy transfer to excited state $^5D_4$, it posses an energy back-flow quenching route [19]. Energy back-flow shortens the decay times with ligands having triplet-state energy levels near the $^5D_4$ level of terbium [9]. It has been also found that those chelates express additionally enhanced environmental sensitivity, and are strongly quenched upon conjugation to proteins [10].

In a number of terbium(III) chelates it has been found, however, that shortening of the decay times is not directly related to respective decrease in quantum yield. An example of an opposite phenomenon is the aliphatic diketone chelates in aqueous solution [20]. Gradual substitution of hydrogen by fluorines from zero to six in 2,4-pentanedione not only increased ligand protonation allowing low pH to be used, but also decreased the decay

times of the respective terbium chelates from 390 μs with pentanedione to 73 μs with trifluorosubstituted and further to 30 μs with hexafluorosubstituted derivatives. The luminescence intensity was, on the contrary, increased by 26- and 32-fold upon fluorination. Similar shortenings of terbium(III) decays, not explained by energy back-flow theory, are found with a number of other structures. The increase of radiative emission rate, so far reported only with lanthanides in close proximity to metallic silver island surfaces [21], could explain some of these observations. Efficient and short decay terbium(III) chelates—together with long decay chelates—would provide valuable additional labels, e.g. for various multiplexing experiments.

Emission Properties

The excited lanthanides express ion-specific luminescence mainly originating from the lowest excited state. Lanthanide emissions are characterized by transitions to ground state manifold resulting in ion- and chelate-specific profile. The ligand field around the ion can change the fine structure of the transition mainly expressed as a change in the relative intensities of the major lines [14] as compared to the other transitions. Controlling of the emission line proportions can be utilized in optimizing total emission integration, to gather maximum amount of light with minimum bandwidth to avoid background interference, and to minimize donor-related background in energy transfer assays (e.g. relative europium emission intensity at 665 used to measure FRET acceptor emission as compared to overall excited state energy).

Emissions emanating from upper excited levels are less intense, but can be recorded with highly luminescent chelates, as exemplified with a europium chelate in Fig. 2. The transition from $^5D_1$ or $^5D_2$ levels have found practical applications in search for new, more sensitive wavelength areas for TR-FRET applications (see section 'Energy Transfer'). The excited state lifetime of $^5D_1$ is at microsecond range, and is found to be independent of triplet quenching oxygen or O—H vibrations [22].

The major emission lines and the respective transitions of the luminescent lanthanides are collected in Table I [1,2,23]. The near infrared (NIR) emitting lanthanides ytterbium, neodymium, holmium, and erbium have recently created interest, not only for telecommunication, but also as red-shifted, medium decay time probes for bioanalytical applications [2,14–18,23]. In addition to red-shifted emission, those lanthanides can also be excited through visible light absorbing ligands. Their practical applications in bioaffinity assays are so far limited by their sub-microsecond decay times and the strong quenching related to their narrow energy gap requiring particularly good shielding system.

Luminescence Quenching

Chelate-bound, inner sphere water molecules (O—H vibrational overtones) is the most common excited state non-radiative relaxation route with all the luminescent lanthanide chelates [24]. The decay differences when measured in deuterium oxide as compared to regular water, is generally used as a measure to ligand coordination number [24]. The Horrocks equation (3) is particularly useful in defining coordination with europium(III) chelates.

$$n = A\left(\tau_{H_2O}^{-1} - \tau_{D_2O}^{-1}\right) \tag{3}$$

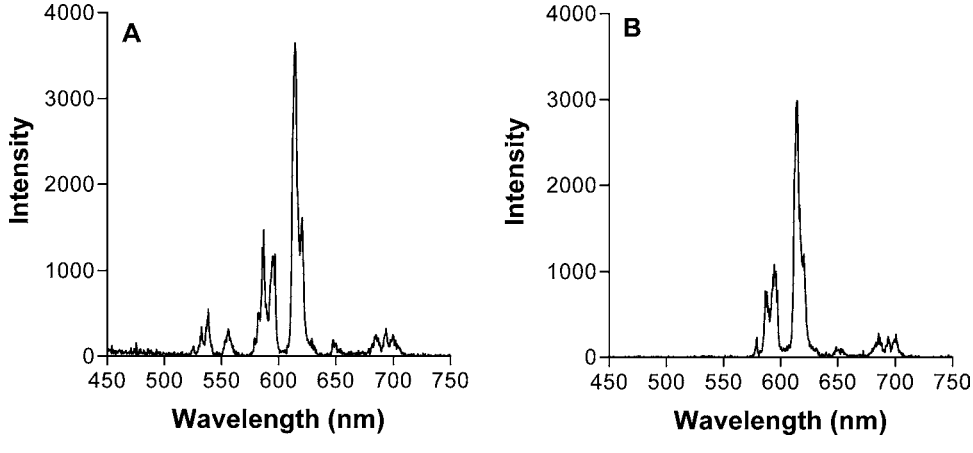

Fig. 2. Eu(III) emission spectrum measured with 2 μs delay time (A) and 7 μs delay time (B). Short delay enables the detection of emittive transitions from $^5D_1$ state (peaks at ~535 nm and 555 nm). The spectra are un-corrected.

where n is the number of coordinated water molecules in the first coordination sphere, A is a lanthanide ion-specific constant (e.g. 1.05 for Eu(III)).

Similarly to inner-sphere water molecules, outer-sphere water also creates luminescence quenching, found as a luminescence enhancement upon drying or upon changing solvent, or when comparing luminescence intensities of nona-dentate chelates in D_2O and H_2O. In addition to O—H vibrational deactivation, also the N—H and C—H vibrations create excitation state deactivations routes [25–27] and recently the Horrocks equation has been refined to take into account also other oscillations [28]. In a fully coordinated europium(III) chelate, replacing the hydrogen atoms by deuterium has been found to increase both the quantum yield and decay time [29].

Europium(III) chelates, due to the existence of two possible oxidation states (III and II), suffer quenching by charge transfer reaction, which is regarded as a major quenching route in some europium(III) chelates [30,31]. Terbium(III) does not possess II state and hence its chelates are not quenched by charge transfer. As stated earlier, terbium, due to its electronic configuration, is quenched by excited state energy back-flow, from excited $^5D_4$ level to ligand triplet state, if their respective energies are partly overlapping [9,11,20].

Luminescence quenching by assay matrix components also has to be taken into considerations in bioanalytical applications [32]. For various applications the sample, e.g. drug screening library compound, can have a strong interference with the measured signal. Sample quenching may take place through Förster-type energy transfer, be related to short distance Dexter type of energy transfer [33], ionic interaction [34], may take place through paramagnetic ions [35], free radicals [37], or metallic surface [37]. In addition, the long excited state lifetime sets additional demand for luminescence due to the longer diffusion time allowed for radiative or non-radiative reactions to take place.

Oxygen, a well known triplet quencher, does not have any strong quenching effect on commonly used lanthanide chelates. Oxygen has higher effect on NIR emitting chelates, but is reported to have negligible effect on e.g. ytterbium(III) chelate due to rapid and efficient triplet to metal energy transfer rate constant [14]. Ionic interaction with charged chelates possibly comprises the most severe interfering factors in homogeneous assays. Positively charged chelates are efficiently quenched by anionic compounds, such as serum uric acid for europium(III) cryptate chelates [34] and respectively negatively charged chelates are sensitive to cationic compounds (such as metallic ions).

Calculated by the basic energy gap criteria, the most luminescent lanthanide after gadolinium would be terbium followed by europium. Samarium and dysprosium, having much more narrow energy gap between the lowest excited level and highest ground state manifold, exhibit less intense and shorter decay emissions. Similarly, the near infrared emitting lanthanides, neodymium, ytterbium and erbium, having very narrow energy gap, exhibit very short decay time emission. In regard to O—H quenching terbium has been shown to be more robust. On the other hand, the short decay luminescent chelates possess less diffusion-related matrix quenching, which in part compensates the gap differences in respect to sample-related interferences [38].

Depending on the assay and measuring configuration, matrix-related interferences may have to be eliminated. In heterogeneous assays interfering matrix-related compounds are generally washed away before measurement, and optimal luminescence conditions are arranged e.g. by using synergistic compounds such as TOPO and Triton [39], urea and SDS [40,41], KCSN and solvent [42] or simply by drying [43,44]. In homogeneous assays, the matrix compounds are present also during measurement. In FRET ratio-fluorometry is one way to avoid major part of interferences because most of the signal interfering reactions take place either at excitation site or at donor site [45]. In addition to the use of ratio between donor and acceptor emissions, analysis of changes of decay times, and excitation attenuation, can be used to gather additional information from the measurement and for deconvolution of the real concentrations [32].

Energy Transfer

Application of probes of different decay times in Förster-type energy transfer assays (TR-FRET) provides a clear advantage over conventional FRET in that the produced energy-transfer derived acceptor emission is distinguished from donor and direct acceptor both in respect to spectral and to temporal characteristics [46]. Lanthanide chelates, due to their line-type emissions and exceptionally long decay times, suit perfectly to TR-FRET [34]. A scheme of TR-FRET with a europium donor is given in Fig. 3.

Luminescent europium(III) chelates are the most commonly used donors in TR-FRET, also commercialized e.g. as TRACE®/Kryptor® system of Brahms, HTRF® of CisBio International, LANCE® by Perkin-Elmer, and in LRET® of Amersham. Europium chelates have very long decay times allowing very simple temporal discrimination between donor, acceptor, and FRET signals. The long decay time also allows efficient dynamic energy transfer

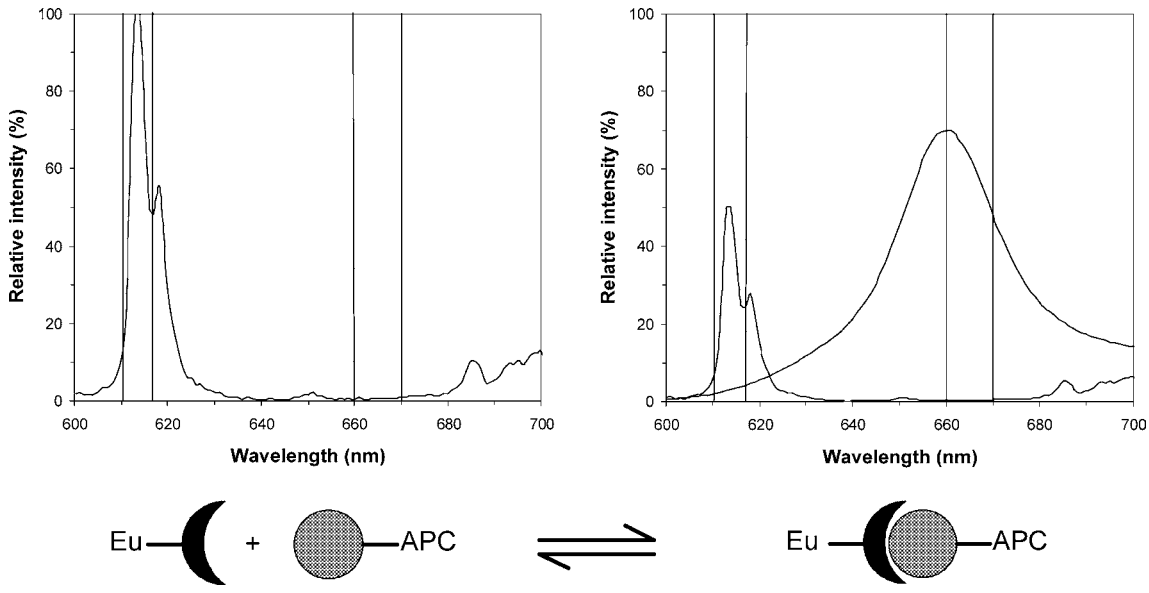

Fig. 3. TR-FRET principle using europium chelates as energy donor and allophycocyanin (APC) as acceptor. Respective filters at 613 and 665 nm used for donor and acceptor measurement are shown by bars.

reactions with flexible complexes, and on the other hand, diminishes orientational factor effect on FRET. The long wavelength emission ensures low background for acceptor measurement (665 nm most generally applied), even though the number of high efficient acceptors are somewhat restricted at that wavelength area. Europium produces typical emission spectrum characterized by several transitions (Fig. 2), from which the magnetical dipole defined transition ($^5D_0$–$^7F_1$) is not regarded as resonance partner [33].

In a study based on a whole series of acceptors of different absorption properties in the range of 600–780 nm, it was found that europium can potentially function as energy donor at its most transitions from $^5D_0$ level [Laitala unpublished data]. In addition to the typically applied $^5D_0$–$^7F_2$ transition (613 nm), also the $^5D_0$–$^7F_4$ transition was found to be efficient donating transition. The NIR lines at 690–710 nm have been applied in TR-FRET for example using Alexa® 680 as acceptor in an assay of estradiol [47].

The most commonly used energy acceptor with europium(III) chelates is allophycocyanin, which due to its very high molar extinction coefficient (700.000) and quantum yield (0.7) results in rather long Förster radius, up to 9 nm [34]. The other acceptors applicable in TR-FRET with europium are Cy-5 [48,49] and its derivatives and to Alexa® dyes 647 [50] and −680 [47]. Those acceptors show reasonable good spectral overlap integral and hence are functioning well even in reasonably long distance assays, such as protein–protein interactions.

In addition to europium(III), terbium(III) has recently found applications in TR-FRET [51–53] and is also commercialized by Invitrogen under the trade name Lanthascreen®. Terbium can donate energy to fluorescein through its first transition ($^5D_4$–$^7F_6$). Terbium is able to transfer energy as well from the second transition ($^5D_4$–$^7F_5$) to Cy-3, phycoerythrin, rhodamine derivatives or respective Alexa® dyes.

The TR-FRET induced acceptor emission has generally a decay directly related to donor decay time and inversely to the energy transfer efficiency. In most of the applications, the relatively long distance e.g. in protein–protein complexes results in low energy transfer efficiency and accordingly relatively long decay time, typically in the range of 100–1000 μs. Such a FRET signal is easily detected with commercially available time-resolving plate fluorometers based on gated detection. The TR-FRET signal is distinguished from background and from directly excited acceptor emission by temporal filtering and from the long decay donor by its red-shifted emission (Fig. 3).

Short distance energy transfer by non-emitting acceptors is generally termed quenching (TR-FQA). TR-FQA has got applications in assays of hydrolysing enzymes, such as proteases, where the flexibility of donor- and quencher-labeled substrate peptides, together with the long donor decay and efficient quenchers, allow highly efficient dynamic quenching and thus monitoring the enzymatic reaction by increasing signal [54]. Different substrate structures require somewhat different designs in respect to quenchers (overlap integral) and quenching

efficiencies. In a study of different types of substrates [55] proteases functioned best with QSY-7 as the quencher, helicase with QSY-7 or dabcyl and phosphatase with Cy-5. Cy-5 is a typical overlapping dye, and was used to label anti-phosphotyrosine antibodies, which upon excessive labeling resulted practically non-fluorescent antibody conjugate.

In addition to europium, also terbium has been used in TR-FQA e.g. in monitoring helicase activity [56]. In protease multiplexing all four luminescent lanthanides, europium, terbium, samarium, and dysprosium have been tested and a triple-label assay was demonstrated for caspases 1, 3, and 6 [57]. Multiplexing is also applied in homogeneous, closed tube DNA hybridization assays using both europium- and terbium chelates with QSY-7 as the generic quencher [58]. Lanthanide chelate based assays allowed direct double-label analysis of genomic sequences (SNP) from whole blood or blood spots in 96- or 384-well plates.

In short distance FRET (e.g. in DNA hybridization assays), the energy transfer efficiency does not necessarily correlate directly to spectral overlapping, but rather to energetic overlapping. The presence of practically non-emittive higher level excited states allows the development of highly sensitive FRET type assays, in which the acceptor emission takes place at a shorter wavelength than the donor emission (anti-Stokes' shift FRET) [59]. In this sort of TR-FRET (nFRET), the induced acceptor emission has multicomponent decay, likely related to the decays of $^5D_1$ or $^5D_2$ states of europium, and the signal behavior is not following the Förster's theory of energy transfer.

Intramolecular energy transfer has also been utilized in making tunable label complexes, tandem-probes composed of europium(III) and Cy-5, or terbium(III) and fluorescein as the acceptor [60]. The decay time was adjustable within the range from 50 to 500 μs by changing the donor–acceptor distance on a nucleotide backbone.

An other 'internal' energy transfer phenomenon used with lanthanide chelates is the chelate-to-chelate energy transfer applied in co-fluorescence enhancement [61–63]. In co-fluorescence-based enhancement system the use of excess of inert metallic ions, such as gadolinium or yttrium, forms small chelate aggregates allowing efficient chelate-to-chelate energy transfer, possibly by ligand triplet level, and the luminescent chelates functions as acceptors whereby showing orders of magnitude increased excitation efficiencies.

NOVEL LANTHANIDE PROBES

The types of chelating ligands developed for lanthanides can be divided by type of application, by chelate formation moiety or by their antenna part [2]. For enhancement-based assays, the labeling ligand does not have to contain light-harvesting part (e.g. Delfia ligands) but its solubility is of prime importance. In these systems the enhancing ligands does not have to be highly water soluble, neither very strong chelating agents [2,39]. Most commonly these enhancement-based assays are composed of polycarboxylate (EDTA, DTPA) based labeling reagents and β-diketone-based chelators in enhancement to create luminescence [1,2].

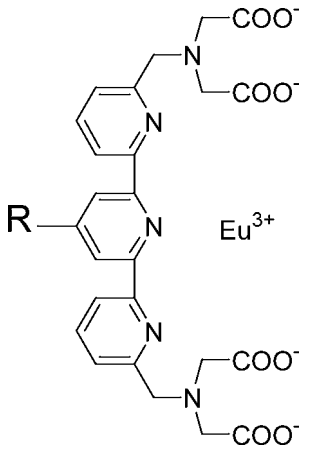

Fig. 4. Structure of a typical luminescent lanthanide chelate composed of terpyridine antenna part, polycarboxylate complexing part and emittive europium ion.

Increasing amount of novel chelate structures has been published in recent years, not reviewed here in detail. Figure 4 shows an example of luminescent lanthanide chelate based on terpyridine as the light harvesting antenna part and polyacids for creating nona-dentate complex. Depending of binding arm position, terpyridine can be used as antenna for europium, samarium, terbium, and dysprosium. The most commonly used antenna moieties are based on pyridine, bipyridine, terpyridine, salicylate, coumarin derivatives, phenanthroline, and various pyrazole derivatives. Also the complexing part varies from polyacid to various forms of macrocycles. Wide variety of published structures has been recently reviewed [2].

One of the recent trends in the field has been the development of various nanobeads composed of latex particles, silica-based beads or inorganic lanthanide doped phosphors. The spectral properties of lanthanides make them particularly well suited for nanobeads due to the lack of inner-filter quenching. The novel nanobead structures allow also the bioassay applications with near-infrared emitting lanthanides, such as neodynium, erbium, praseodynium, holmium, and ytterbium [18].

Qian *et al.* [64] described the development of latex bead system composed of thenoyltrifluoroacetone

europium chelates. Similar nanobeads have since become commercially available, e.g. from Serono Inc., and used e.g. in highly sensitive immunoassays [65–67]. Latex beads modified with polyethylene glycol (PEG) have been used in highly sensitive time-resolved fluorometric immunoassay down to the level of zeptomolar sensitivity [68].

Silica-based nanobeads functionalized for coupling and containing stable lanthanide chelates [69] or tetradentate β-diketones [70] have been developed and used in sensitive immunoassays. Europium-labeled nanobeads are also used as TR-FRET donors. The high background derived from excessive chelates was avoided using relatively small beads and near-infrared acceptors [47].

APPLICATIONS

Lanthanide chelates have found applications in various fields of biomedical assays starting form radiotheraphy based on some samarium isotopes, nuclear magnetic imaging (MRI) [71], specific cleavage of DNA or RNA, and for sensing of various analytes and conditions. Europium chelate have been used for sensing pH [72], temperature [73], light doses, phosphate with unsaturated europium chelate [74], glucose by time-resolved imaging [75], catalase by using tetracycline as enhancing ligand [76], neurotoxic agents for bioterror monitoring [77], and anestethic agent using a dried strip reagent [78]. In bioanalytical assays, the photoluminescent lanthanides have the largest applications, even though terbium is also used in time-resolved electroluminometric assays [79].

Immunoassays

The first bioanalytical applications of lanthanide chelates were in the field of clinical immunodiagnostics, and even to day that is the topic of most of the published applications and several commercial product lines. Two of the most frequently applied technologies are DELFIA®, a heterogeneous assay technology based on fluorescence enhancement from Perkin-Elmer [39] and homogeneous TR-FRET (TRACE®) of Brahms. Some examples of the most recent applications are e.g. diabetes-related autoantibody assays [80,81], assay of kallikrein for prostate screening [82] and hyaluronan assay [83]. For nutritional analytes, Delfia has been used for analysis of various sulfonamides [84], prion protein (PrP^c) on animal tissues [85] and *E. coli* caused colitis in cider [86]. Enterolactones and phytoestrogens are analyzed in serum as markers for healthy food and prognosis of cancers [87,88]. In celiac research, Delfia has been applied to study transglutaminase activity based on gliadin substrate [89]. Detection of different infectious microbes as potential terror and warfare agents have been developed for monitoring biohazard [90].

Stable luminescent chelates and direct surface measurement has recently been reported e.g. in assays of insulin [91], TSH [92], Hepatitis B surface antigen [70], a herbicide atrazine [93] and PSA [65,66,69] using beads. TR-FRET technology has been reported for PAPP-A [94], microalbumin in urea [67], and 17-β estradiol using nanobeads as europium containing acceptors [71].

Molecular Diagnostics

Molecular diagnostics assays are mainly used today to analyze microbes, such as streptococcus [95], but are gaining interest in respect to pharmacogenomics, personalized medicine and for genetic testing of predisposition to diseases. In addition to more conventional detection principles, such as Delfia used for example analysis of Factor V Leiden mutation [96], various forms of TR-FRET and TR-FQA are applied for more convenient homogeneous PCR detection assays. Lanthanides provide good sensitivity and a wide variety of opportunities to do also focused multiplexing. A method to label oligonucleotides with luminescent chelates during synthesis has been developed to simplify labeling [97].

Use of two or more lanthanides simultaneously is applied for PCR detection of diabetes susceptibility [98], bacterial toxin related gene detection [99] and seven-color hybridization assay of papilloma virus types using combination of three lanthanides [100]. In prostate screening, PSA-related mRNA was detected from periferal blood samples with reverse transcription and europium chelate-labeled probes [101].

Tsourkas *et al*. used DTPA-cs124 chelate in a dual-label TR-FRET hybridization assay based on two beacon-type probes labeled with dancyl as a quencher and either with europium or terbium chelates as donors [102]. Matsumoto *et al*. used a terbium chelate together with Cy-3 in a TR-FRET hybridization assay [103].

Luminescence quenching assay based on short oligonucleotide sequences labeled with a generic quencher has been used to develop TR-FQ assays for PCR quantitation [58,104,105]. The technology allows focused multiplexing and totally integrated closed tube analysis. In addition, the possibility to control proximity allows highly efficient energy transfer assays. The non-overlapping type of TR-FRET can be applied to further improve sensitivity in hybridization assays [59].

Drug Discovery Applications

In drug discovery, and in particular in the primary screening (high-throughput screening), there is a need for sensitive, robust and preferable homogeneous assay technology. That is why a number of commercial vendors have begin to utilize stable fluorescent lanthanide chelates and energy transfer-based technologies for drug discovery, including CisBio International HTRF, Invitrogen Lanthascreen, Amersham LRET, and Perkin-Elmer Lance TR-FRET, and TruPoint TR-FQA technologies.

Receptors, and G-protein coupled receptor in particular, create the largest group of drug targets. Receptor–ligand interaction is the first step in cellular signal transduction, exemplified with Delfia assays of MHC binding [106], α-MSH [107], and androgens [108]. Ligand stimulated receptor activation has also been followed by thermoimaging by utilizing europium-threnoyltrifluoroacetone as temperature sensitive probes [109].

Since the receptor activation, a wide variety of secondary functional assays are applied to follow downs stream signaling. For example GTP binding can be followed with europium-labeled GTP [110]. Various kinases are the next largest target group, and very widely analyzed in screening with various lanthanide-based technologies, both heterogeneous and homogeneous by various combinations of TR-FRET technologies. Recent examples include serine/threonine kinases [111,112] and use of sol–gel for kinase sensing by TR-FRET [113]. Sadler *et al.* compared Delfia to TR-FRET in I kappa B kinase [114] and Minor studied receptor phosphorylation with Delfia [115]. TR-FRET assay on a flow injection analysis is applied for measuring epidermal growth factor receptor kinase with europium cryptate and APC derivative as acceptor [116].

Protein–protein interaction is most commonly measured by FRET, and improved by use of lanthanide labels in TR-FRET [117–119]. Receptor dimerization or oligomerization have quite recently found to be an important signal transduction and controlling mechanism, analyzed commonly by TR-FRET [120–123]. Nuclear receptor coactivator recruitment assays relate to downstream signaling cascades at nuclear level [124,125] exemplified by hypoxia induced factor binding to p300 transcription coactivator [126].

Antigen stimulated cytokine release by T cells [127] as well as expression of three adhesion markers is accomplished by triple-label assay using europium, terbium, and samarium in Delfia technology [128] and interferon-γ production by TR-FRET [129]. TR-FRET has been used also for bacterial transcription assays [130,131]. Heat shock protein inhibition assays [132–134] and tumor suppression by cellular quantitation of pRb phosphorylation [135] by Delfia technology.

Besides kinases and phosphatase, various other enzymes, in particular proteases, create an important target group and application field for lanthanide-based screening assays. Apoptotic cell death assays by following caspases have been developed by TR-FQ technology [54,55,57] performed also in microspot format having 8640 compound spots on planar plate [136]. In addition to TR-FQA, also TR-FRET has been applied for caspase assays [137] and well as for BACE (β-secretase) related to Alzheimer disease [138]. Other TR-FRET enzyme assays recently published include telomerase (TRAP) [139], helicases [49,56], ubiquitin transferases assays [140,141], and HIV proteases [142].

Drug discovery and subsequent ADME and toxicity studies are becoming a bottleneck in drug discovery process. Therefore, there is a tendency towards more cellular and more functional assays. Cytotoxicity and natural killer cell activity measurements are traditionally done with radioactive chromium release test, which can be replaced with non-radiative alternatives based on lanthanides, such as europium release [143] or by using fluorogenic chelating ligand (BADTA, Perkin-Elmer) release [144]. In cell-based assays, phosphorylation can be analyzed on cellular environment [145]. Somjen *et al.* studied estrogen receptor response on bone cells using europium-labeled estradiol [146]. Vesicle transport has been studied using a membrane soluble europium chelate [147]. Chakrabasty studied myosin rod arrangements with TR-FRET [148] and Becker *et al.* [149] studied ion channel in *E. coli* model using TR-FRET technique.

Use of europium has been found very useful also in pharmacokinetic studies of drug transportation and accumulation [150]. Europium-labeled albumin was recently used to study blood–brain barrier function during experimental meningitis [151].

Long decay time lanthanides, in a form of phosphors, beads, or stable chelates, have also created interest in imaging [2]. In addition to autofluorescence elimination, the use of different set of labels, lanthanide chelates together with Pt/Pd porphyrins which can be imaged at millisecond time domain and regular fluorochromes imaged at regular prompt domain, allows multiplexing, e.g. in differential cell counting and cellular applications [152].

CONCLUSION

The advent of highly luminescent lanthanides, long decay probes optimized for various properties, are rapidly

expanding the applications of lanthanides for a wide variety of bioanalytical assays. In addition to providing robust, background-free detection in heterogeneous assays, they allow robust detection also for homogeneous assays. The spectrally and temporally defined emission properties can be exploited in multiplexing. In various forms of energy transfer technologies there is a choice of lanthanide donors and for each of them there are a variety of available acceptors. The acceptors can produce emissions from the anti-Stokes' shift area below the donor emission up to near infrared area, and each of those signals can have their specific lifetimes adjusted by the specific proximity in the assay.

REFERENCES

1. I. Hemmilä (1990). *Applications of Fluorescence in Immunoassays*, Wiley Interscience, New York.
2. I. Hemmilä and V.-M. Mukkala (2001). Time-resolution in fluorometry technologies, labels and applications in bioanalytical assays. *Crit. Rev. Clin. Lab. Sci.* **38**, 441–519.
3. W. T. Carnall, P. R. Fields, and K. Rajnak (1968). Electronic energy levels in the trivalent lanthanide aquo ions. I. Pr^{3+}, Nd^{3+}, Pm^{3+}, Sm^{3+}, Dy^{3+}, Ho^{3+}, Er^{3+}, and Tm^{3+}. *J. Chem. Phys.* **49**, 4424–4442.
4. W. T. Carnall, P. R. Fields, and K. Rajnak (1968). Electronic energy levels in the trivalent lanthanide aquo ions II. Gd^{3+}. *J. Chem. Phys.* **49**, 4443–4446.
5. W. T. Carnall, P. R. Fields, and K. Rajnak (1968). Electronic energy levels in the trivalent lanthanide aquo ions. III. Tb^{3+}. *J. Chem. Phys.* **49**, 4447–4449.
6. W. T. Carnall, P. R. Fields, and K. Rajnak (1968). Electronic energy levels of the trivalent lanthanide aquo ions. IV. Eu^{3+}. *J. Chem. Phys.* **49**, 4450–4455.
7. S. I. Weissman (1942). Intramolecular energy transfer, the fluorescence of complexes of europium, *J. Chem. Phys.* **10**, 214–217.
8. H. Lemmetyinen, E. Vuorimaa, A. Jutila, V. M. Mukkala, H. Takalo, and J. Kankare (2000). A time-resolved study of the mechanism of the energy transfer from a ligand to the lanthanide(III) ion in solution and solid films. *Luminescence* **15**, 341–350.
9. M. Latva, H. Takalo, V. M. Mukkala, C. Matachescu, J. C. Rodrígues-Ubis, and J. Kankare (1997). Correlation between the lowest triplet state energy level of the ligand and lanthanide(III) luminescence quantum yield. *J. Luminesc.* **75**, 149–169.
10. I. Hemmilä, V.-M. Mukkala, and H. Takalo (2005). Development of luminescent lanthanide chelate labels for diagnostic assays. *J. Alloys Compounds* **249**, 158–162.
11. F. Gutierrez, C. Tedeschi, L. Maron, J. P. Daudey, R. Poteau, J. Azema, P. Tisnes, and C. Picard (2004). Quantum chemistry-based interpretations on the lowest triplet state of luminescent lanthanides complexes. Part 1. Relation between the triplet state energy of hydroxamate complexes and their luminescence properties. *Dalton Trans.* 1334–1347.
12. A. Dadabhoy, S. Faulkner, and P. G. Sammes (2005). Small singlet–triplet energy gap of acridone enables longer wavelength sensitization of europium(III) luminescence. *J. Chem. Soc. Perkin Trans.* **2**, 2359–2360.
13. F. R. G. Silva and O. L. Malta (1997). Calculation of the ligand-lanthanide ion energy transfer rate in coordination compounds: Contributions of exchange interactions. *J. Alloys Compounds* **250**, 427–430.
14. J.-C. Bünzli and G. R. Chopin (1989). *Lanthanide Probes in Life, Chemical and Earth Sciences. Theory and Practice*, Elsevier, Amsterdam, New York.
15. M. H. Werts, R. H. Woudenberg, P. G. Emmerink, R. van Gassel, J. W. Hofstraat, and J. W. Verhoeven (2000). A near-infrared luminescent label based on Yb(III) ions and its application in a fluoroimmunoassay. *Angew. Chem. Int. Ed. Engl.* **39**, 4542–4544.
16. M. H. Werts, J. W. Hofstraat, F. A. J. Geurts, and J. W. Verhoeven (1997). Fluorescein and eosin as sensitizing chromophores in near-infrared luminescent ytterbium(III), neodynium(III) and erbium(III) chelates. *Chem. Phys. Lett.* **276**, 196–201.
17. S. Faulkner, A. Beeby, R. S. Dickins, D. Parker, and J. A. G. Williams (1999). Generating a warm glow: Lanthanide complexes which luminescence in the near-IR. *J. Fluorescence* **9**, 45–49.
18. F. C. van Veggel, J. W. Stouwdam, G. A. Hebbink, and J. Huskens (2003). Lanthanide(III)-dobed nanoparticles that emit in the near infrared. *Proc. SPIE* **5224**, 164–175.
19. N. Sabbatini and M. Guardigli (1993). Luminescent lanthanide complexes as photochemical supramolecular devices. *Coord. Chem. Rev.* **123**, 201–228.
20. I. Hemmilä (1985). Time-resolved fluorometric determination of terbium in aqueous solution. *Anal. Chem.* **57**, 1676–1681.
21. J. R. Lakowicz, B. P. Maliwal, J. Malicka, Z. Gryczynski, and I. Gryczynski (2002). Effects of silver island films on the luminescent intensity and decay times of lanthanide chelates. *J. Fluorescence* **12**, 431–437.
22. A. Beeby, S. Faulkner, D. Parker, and J. A. G. Williams (2001). Sensitized luminescence from phenanthridine appended lanthanide complexes: Analysis of triplet mediated energy transfer processes in terbium, europium and neodynium complexes. *J. Chem. Soc. Perkin Trans.* **2**, 1268–1273.
23. S. Faulkner, M. C. Carrie, S. J. A. Pope, J. Squire, A. Beeby, and P. G. Sammes (2004). Pyrene-sensitised near-IR luminescence from ytterbium and neodymium complexes. *Dalton Trans.* 1405–1409.
24. W. De. W. Horrocks Jr. and D. R. Sudnick (1979). Lanthanide ion probes of structure in biology. Laser-induced luminescence decay constants provide a direct measure of the number of metal-coordinated water molecules. *J. Am. Chem. Soc.* **101**, 334–340.
25. S. Lis (2002). Luminescence spectroscopy of lanthanide(III) ions in solution. *J. Alloys Compounds* **341**, 45–50.
26. G. E. Buono-Cuore, H. Li, and B. Arciniac (2005). Quenching of excited states by lanthanide ions and chelates in solution. *Coord. Chem. Rev.* **99**, 55–87.
27. A. Beeby, I. M. Clarkson, R. S. Dickins, S. Faulkner, D. Parker, L. Royle, A. S. de Sousa, J. A. G. Williams, and M. Woods (1999). Non-radiative deactivation of the excited states of europium, terbium and ytterbium complexes by proximate energy-matched OH, NH and CH oscillators: An improved luminescence method for establishing solution hydration states. *J. Chem. Soc. Perkin Trans.* **2**, 493–504.
28. R. M. Supkowski and W. D. Horrocks Jr. (2002). On the number of water molecules, q, coordinated to europium(III) ions in solution from luminescence decay lifetimes. *Inorg. Chim. Acta* **340**, 44–48.
29. I. Hemmilä, V.-M. Mukkala, and H. Takalo (1997). Development of luminescent lanthanide chelate labels for diagnostic assays. *J. Alloys Compounds* **249**, 158–162.
30. N. Sabbatini (1987). Radiative and nonradiative transitions in the Eu(III) hexaaza macrocyclic complex $[Eu(C_{22}H_{26}N_6)(CH_3COO)](CH_3COO)\ Cl{\cdot}2H_2O$. *J. Chem. Phys.* **91**, 4681–4685.
31. S. Petoud, J.-C. Bünzli, T. Glanzman, C. Piguet, Q. Xiang, and R. P. Thummel (1999). Influence of charge-transfer states on the Eu(III) luminescence in mononuclear triple helical complexes with tridentate aromatic ligands. *J. Luminescence* **82**, 69–79.
32. I. Hemmilä (1999). LANCE^{TM}: Homogeneous assay platform for HTS. *J. Biomol. Screen.* **4**, 303–308.
33. D. L. Dexter (1953). A theory of senritized luminescence in solids. *J. Chem. Phys.* **21**, 836–850.
34. G. Mathis (1993). Rare earth cryptates and homogeneous fluoroimmunoassays with human sera. *Clin. Chem.* **39**, 1953–1959.

35. N. Sabbatini, S. Perathoner, G. Lattanzi, S. Dellonte, and V. Balzani (1988). Electron- and energy-transfer processes involving excited states of lanthanide complexes: Evidence for inner-sphere and outer-sphere mechanism. *Inorg. Chem.* **27**, 1628–1633.
36. J. Matko, A. Jenei, T. Wei, and M. Edidin (1995). Luminescence quenching by long range electron transfer: A probe of protein clustering and conformation at the cell surface. *Cytometry* **19**, 191–200.
37. V. H. Perez-Luna, S. Yang, E. M. Rabinovich, T. Buranda, L. A. Sklar, P. D. Hampton, and G. P. Lopez (2002). Fluorescence biosensing strategy based on energy transfer between fluorescently labeled receptors and a metallic surface. *Biosens. Bioelectron.* **17**, 71–78.
38. L. Stryer, D. D. Thomas, and C. F. Meares (1982). Diffusion-enhanced fluorescence energy transfer. *Annu. Rev. Biophys. Bioeng.* **11**, 203–222.
39. I. Hemmilä, S. Dakubu, V. M. Mukkala, H. Siitari, and T. Lovgren (1984). Europium as a label in time-resolved immunofluorometric assays. *Anal. Biochem.* **137**, 335–343.
40. J. Kropf, E. Quitte, and A. M. Gressner (1991). Time-resolved immunofluorometric assays with measurement of a europium chelate in solution: Application for sensitive determination of fibronectin. *Anal. Biochem.* **197**, 258–265.
41. J. Yuan and K. Matsumoto (1997). Synthesis of a new tetradentate β-diketonate-europium chelate and its application for time-resolved fluorometry of albumin. *J. Pharm. Biomed. Anal.* **15**, 1397–1403.
42. K. Mitrunen, K. Pettersson, T. Piironen, T. Björk, H. Lilja, and T. Lövgren (1997). Dual-label one-step immunoassay simultaneous measurement of free and total prostate-specific antigen concentrations and ratios in serum. *Clin. Chem.* **41**, 115–120.
43. I. Hemmilä and A. Båtsman (1988). Time-resolved immunofluorometry of hCG. *Clin. Chem.* **34**, 1163.
44. P. von Lode, J. Rosenberg, K. Pettersson, and H. Takalo (2003). A europium chelate for quantitative point-of-care immunoassays using direct surface measurement. *Anal. Chem.* **75**, 3193–3201.
45. C. S. Lim, J. N. Miller, and J. W. Bridges (1980). Energy-transfer immunoassay: A study of the experimental parameters in an assay for human serum albumin. *Anal. Biochem.* **108**, 176–184.
46. L. E. Morrison (1988). Time resolved detection of energy transfer: Theory and application to immunoassays. *Anal. Biochem.* **174**, 101–120.
47. L. Kokko, K. Sandberg, T. Lovgren, and T. Soukka (2004). Europium(III) chelate-dyed nanoparticles as donors in a homogeneous proximity-based immunoassay for estradiol. *Anal. Chim. Acta* **503**, 155–162.
48. T. Heyduk and E. Heyduk (2001). Luminescence energy transfer with lanthanide chelates: Interpretation of sensitized acceptor decay amplitudes. *Anal. Biochem.* **289**, 60–67.
49. S. G. Jones, D. Y. Lee, J. F. Wright, J. N. Jones, M. L. Teear, S. J. Gregory, and D. D. Burns (2001). Improvements in the sensitivity of time resolved fluorescence energy transfer assays. *J. Fluorescence* **11**, 13–21.
50. D. Maurel, J. Kniazeff, G. Mathis, E. Trinquet, J. P. Pin, and H. Ansanay (2004). Cell surface detection of membrane protein interaction with homogeneous time-resolved fluorescence resonance energy transfer technology. *Anal. Biochem.* **329**, 253–262.
51. M. Li and P. R. Selvin (1997). Amine-reactive forms of a luminescent diethylenetriaminepentaacetic acid chelate of terbium and europium: Attachment to DNA and energy transfer measurements. *Bioconjugate Chem.* **8**, 127–132.
52. P. R. Selvin, T. M. Rana, and J. E. Hearst (1994). Luminescence resonance energy transfer. *J. Am. Chem. Soc.* **116**, 6029–6030.
53. K. Blomberg, P. Hurskainen, and I. Hemmilä (1999). Terbium and rhodamine as labels in a homogeneous time-resolved fluorometric energy transfer assay of the β subunit of human chorionic gonadotropin in serum. *Clin. Chem.* **45**, 855–861.
54. J. Karvinen, P. Hurskainen, S. Gopalakrishnan, D. Burns, U. Warrior, and I. Hemmila (2002). Homogeneous time-resolved fluorescence quenching assay (Lance) for caspase-3. *J. Biomol. Screen* **7**, 223–231.
55. J. Karvinen, V. Laitala, M. L. Makinen, O. Mulari, J. Tamminen, J. Hermonen, P. Hurskainen, and I. Hemmila (2004). Fluorescence quenching-based assays for hydrolyzing enzymes. Application of time-resolved fluorometry in assays for caspase, helicase, and phosphatase. *Anal. Chem.* **76**, 1429–1436.
56. D. L. Earnshaw and K. J. Moore (2004). Time-resolved fluorescence energy transfer DNA helicase assays for high throughput screening. *J. Biomol. Screen.* **4**, 239–248.
57. J. Karvinen, A. Elomaa, M. L. Makinen, H. Hakala, V. M. Mukkala, J. Peuralahti, P. Hurskainen, J. Hovinen, and I. Hemmila (2004). Caspase multiplexing: Simultaneous homogeneous time-resolved quenching assay (TruPoint) for caspases 1, 3, and 6. *Anal. Biochem.* **325**, 317–325.
58. A. Ylikoski, A. Elomaa, P. Ollikka, H. Hakala, V. M. Mukkala, J. Hovinen, and I. Hemmila (2004). Homogeneous time-resolved fluorescence quenching assay (TruPoint) for nucleic acid detection. *Clin. Chem.* **50**, 1943–1947.
59. V. Laitala and I. Hemmilä (2005). Homogeneous assay based on anti-stokes' shift time-resolved fluorescence resonance energy-transfer measurement. *Anal. Chem.* **77,** 1483–1487.
60. J. Chen and P. R. Selvin (2000). Lifetime- and color-tailored fluorophores in the micro- to millisecond time regime, *J. Am. Chem. Soc.* **122**, 657–660.
61. Y.-Y. Xu, I. Hemmilä, and T. Lövgren (1992). Co-fluorescence effect in time-resolved fluoroimmunoassays. A review. *Analyst* **117**, 1061–1069.
62. Y.-Y. Xu and I. Hemmilä (1992). Co-fluorescence enhancement system based on pivaloyltrifluoroacetone and yttrium for the simultaneous detection of europium, terbium, samarium, and dysprosium. *Anal. Chim. Acta* **256**, 9–16.
63. Y.-Y. Xu, K. Pettersson, K. Blomberg, I. Hemmila, H. Mikola, and T. Lovgren (1992). Simultaneous quadruple-label fluorometric immunoassay of thyroid-stimulating hormone, 17α-hydroxyprogesterone, immunoreactive trypsin, and creatine kinase MM isoenzyme in dried blood spots. *Clin. Chem.* **38**, 2038–2043.
64. D.-J. Qian, H.-G. Liu, H.-X. Huang, Q. Fu, and X.-S. Feng (2001). Europium complex nanoparticles: Preparation, characterization and optical properties. *Mater. Lett.* **51**, 525–528.
65. H. Härmä, T. Soukka, and T. Lövgren (2001). Europium nanoparticles and time-resolved fluorescence for ultrasensitive detection of prostate-specific antigen. *Clin. Chem.* **47**, 561–568.
66. T. Soukka, K. Antonen, H. Harma, A. M. Pelkkikangas, P. Huhtinen, and T. Lovgren (2003). Highly sensitive immunoassay of free prostate-specific antigen in serum using europium(III) nanoparticle label technology. *Clin. Chim. Acta* **328**, 45–58.
67. Q.-P. Qin, T. Lövgren, and K. Pettersson (2001). Development of highly fluorescent detection reagent for the construction of ultrasensitive immunoassays. *Anal. Chem.* **73**, 1521–1529.
68. T. Matsuya, S. Tashiro, N. Hoshino, N. Shibata, Y. Nagasaki, and K. Kataoka (2003). A core-shell type fluorescent nanosphrere possessing reactive poly(ethylene glycol) tethered chains on the surface for zeptomole detection of protein in time-resolved fluorometric immunoassays. *Anal. Chem.* **75**, 6124–6132.
69. Z. Ye, M. Tan, G. Wang, and J. Yuan (2004). Preparation, characterization, and time-resolved fluorometric application of silica-coated terbium(III) fluorescent nanoparticles. *Anal. Chem.* **76**, 513–518.
70. X. Hai, M. Tan, G. Wang, Z. Ye, J. Yuan, and K. Matsumoto (2004). Preparation and a time-resolved fluoroimmunoassay application of new europium fluorescent nanoparticles. *Anal. Sci.* **20**, 245–246.
71. E. Kahn, C. Tessier, G. Lizard, A. Petiet, J. C. Bernengo, D. Coulaud, C. Fourre, F. Frouin, O. Clement, J. R. Jourdain, E. Delain, F. Guiraud-Vitaux, N. Colas-Linhart, N. Siauve, C. A. Cuenod, G. Frija, and A. Todd-Pokropek (2003). Analysis of the distribution of MRI contrast agents in the livers of small animals by means of complementary microscopies. *Cytometry A* **51**, 97–106.
72. A. Lobnik, N. Majeen, K. Niederkiter, and G. Uray (2001). Optical pH sensor based on the absorption of antenna generated europium

luminescence by bromothymolblue in a sol–gel membrane. *Sens. Actuators B* **74**, 200–206.
73. G. E. Khalil (2004). Europium β-diketonate temperature sensors: Effects of ligands, matrix, and concentration. *Rev. Sci. Instrum.* **75**, 192–206.
74. S.-H. Li, W. T. Yuan, C. Q. Zhu, and J. G. Xu (2004). Species-differentiable sensing of phosphate-containing anions in neutral aqueous solution based on coordinatively unsaturated lanthanide complex probes. *Anal. Biochem.* **331**, 235–242.
75. M. Schafering, M. Wu, and O. S. Wolfbeis (2004). Time-resolved fluorescent imaging of glucose. *J. Fluorescence* **14**, 561–568.
76. M. Wu, Z. Lin, and O. S. Wolfbeis (2003). Determination of the activity of catalase using a europium(III)-tetracycline-derived fluorescence substrate. *Anal. Biochem.* **320**, 129–135.
77. J. C. DiCesare, J. Parker, S. N. Horne, J. Kita, R. Earni, and C. Peeples (2004). Progress in developing nerve agent sensors using combinatorial technique. *Mat. Res. Soc. Symp. Proc.* **787**, 17–22.
78. A.-M. Casas-Hernandez, M. P. Aguilar-Caballos, and A. Gomez-Hens (2002). Application of time-resolved luminescence methodology to the determination of phthalate esters. *Analytical letters* **36**, 1017–1027.
79. S. Kulmala, M. Hakansson, A. M. Spehar, A. Nyman, J. Kankare, K. Loikas, T. Ala-Kleme, and J. Eskola (2002). Heterogeneous and homogeneous electrochemiluminoimmunoassays of hTSH at disposeable oxide-covered aluminum electrodes. *Anal. Chim. Acta* **458**, 271–280.
80. A. Westerlund-Karlsson, K. Suonpaa, M. Ankelo, J. Ilonen, M. Knip, and A. E. Hinkkanen (2003). Detection of autoantibodies to protein tyrosine phosphatase-like protein IA-2 with a novel time-resolved fluorimetric assay. *Clin. Chem.* **49**, 916–923.
81. M. Ankelo, A. Westerlund-Karlsson, J. Ilonen, M. Knip, K. Savola, P. Kankaanpaa, L. Merio, H. Siitari, and A. Hinkkanen (2003). Time-resolved fluorometric assay for detection of autoantibodies to glutamic acid decarboxylase (GAD65). *Clin. Chem.* **49**, 908–915.
82. A. Haese, V. Vaisanen, J. A. Finlay, K. Pettersson, H. G. Rittenhouse, A. W. Partin, D. J. Bruzek, L. J. Sokoll, H. Lilja, and D. W. Chan (2003). Standardization of two immunoassays for human glandular kallikrein 2. *Clin. Chem.* **49**, 601–610.
83. J. R. Martins, C. C. Passerotti, R. M. Maciel, L. O. Sampaio, C. P. Dietrich, and H. B. Nader (2003). Practical determination of hyaluronan by a new noncompetitive fluorescence-based assay on serum of normal and cirrhotic patients. *Anal. Biochem.* **319**, 65–72.
84. T. Korpimaki, V. Hagren, E. C. Brockmann, and M. Tuomola (2004). Generic lanthanide fluoroimmunoassay for the simultaneous screening of 18 sulfonamides using an engineered antibody. *Anal. Chem.* **76**, 3091–3098.
85. I. R. MacGegor and O. Drummond (2001). Species differences in the blood content of the normal cellular isoform of prion protein, PrPc, measured by time-resolved fluoroimmunoassay Vox. *Sang.* **81**, 236–240.
86. L. S. Yu, S. A. Reed, and M. H. Golden (2002). Time-resolved fluorescence immunoassay (TRFIA) for the detection of *Escherichia coli* O157:H7 in apple cider. *J. Microb. Methods* **49**, 63–68.
87. A. Kilkkinen, K. Stumpf, P. Pietinen, L. M. Valsta, H. Tapanainen, and H. Adlercreutz (2001). Determinants of serum enterolactone concentration. *Am. J. Clin. Nutr.* **73**, 1094–1100.
88. E. Brouwers, R. L'homme, N. Al Maharik, O. Lapcik, R. Hampl, K. Wahala, H. Mikola, and H. Adlercreutz (2003). Time-resolved fluoroimmunoassay for equol in plasma and urine. *J. Steroid Biochem. Mol. Biol.* **84**, 577–587.
89. H. Skovbjerg, O. Noren, D. Anthonsen, J. Moller, and H. Sjöström (2002). Gliadin is a good substrate of several transglutaminase: Possible implication in the pathogenesis of coeliac disease. *Scand. J. Gastroenterol.* **37**, 812–817.
90. A. H. Peruski, L. H. Johnson III, and L. F. Persuki Jr. (2002). Rapid and sensitive detection of biological warfare agents using time-resolved fluorescence assay. *J. Immunol. Methods* **263**, 35–41.
91. J. Yuan, M. Tan, and G. Wang (2004). Synthesis and luminescence properties of lanthanide(III) chelates with polyacid derivatives of thienyl-substituted terpyridine analogues. *J. Luminesc.* 10691.
92. A.-M. Pelkkikangas (2004). Simple, rapid, and sensitive thyroid-stimulating hormone immunoassay using europium(III) nanoparticle label. *Anal. Chim. Acta* **517**, 169–176.
93. J. Feng, S. Guomin, A. Maquieira, M. E. Koivunen, B. Guo, B. D. Hammock, and I. M. Kennedy (2003). Functionalized europium oxide nanoparticles used as a fluorescent label in an immunoassay for atrazine. *Anal. Chem.* **75**, 5282–5286.
94. G. C. Smith, E. J. Stenhouse, J. A. Crossley, D. A. Aitken, A. D. Cameron, and J. M. Connor (2002). Early-pregnancy origins of low birth weight. *Nature* **417**, 916.
95. S. Rintamaki, A. Saukkoriipi, P. Salo, A. Takala, and M. Leinonen (2002). Detection of *Streptococcus pneumoniae* DNA by using polymerase chain reaction and microwell hybridization with europium-labelled probes. *J. Microbiol. Methods* **50**, 313–318.
96. C. G. Potter, Y. T. Liu, and D. C. Rees (2001). Factor V Leiden mutation screened by PCR and detected with lanthanide-labeled probes. *Genet. Test.* **5**, 291–297.
97. H. Hakala, P. Ollikka, J. Degerholm, and J. Hovinen (2002). Oligonucleotide conjugates based on acyclonucleotides and their use in DNA hybridization assays. *Tetrahedron* **58**, 8771–8777.
98. M. Sjoroos, J. Ilonen, H. Reijonen, and T. Lovgren (1998). Time-resolved fluorometry based sandwich hybridization assay for HLA-DQA1 typing. *Dis. Markers* **14**, 9–19.
99. K. Watanabe, H. Arakawa, and M. Maeda (2002). Simultaneous detection of two verotoxin genes using dual-label time-resolved fluorescence immunoassay with duplex PCR. *Luminescence* **17**, 123–129.
100. M. Samiotaki, M. Kwiatkowski, N. Ylitalo, and U. Landegren (1997). Seven-color time-resolved fluorescence hybridization analysis of human papilloma virus types. *Anal. Biochem.* **253**, 156–161.
101. R. Kurek, A. Ylikoski, H. Renneberg, L. Konrad, G. Aumuller, S. J. Roddiger, N. Zamboglou, U. W. Tunn, and H. Lilja (2003). Quantitative PSA RT-PCR for preoperative staging of prostate cancer. *Prostate* **56**, 263–269.
102. A. Tsourkas, M. A. Behlke, Y. Xu, and G. Bao (2003). Spectroscopic features of dual fluorescence/luminescence resonance energy-transfer molecular beacons. *Anal. Chem.* **75**, 3697–3703.
103. K. Matsumoto, T. Nojima, H. Sano, and K. Majima (2002). Fluorescent lanthanide chelates for biological systems. *Macromol. Symp.* **186**, 2001–2121.
104. J. Nurmi, M. Kiviniemi, M. Kujanpää, M. Sjoroos, J. Ilonen, and T. Lövgren (2002). High-throughput genetic analysis using time-resolved fluorometry and closed-tube detection. *Anal. Biochem.* **299**, 211–217.
105. J. Nurmi, T. Wikman, M. Karp, and T. Lovgren (2002). High-performance real-time quantitative RT-PCR using lanthanide probes and a dual temperature hybridization assay. *Anal. Chem.* **74**, 3525–3532.
106. X. Gao, C. K. Hsu, L. J. Heinz, J. Morin, Y. Shi, N. K. Shukla, D. L. Smiley, J. Xu, B. Zhong, and L. J. Slieker (2004). Europium-labeled melanin-concentrating hormone analogues: Ligands for measuring binding to melanin-concentrating hormone receptors 1 and 2. *Anal. Biochem.* **328**, 187–195.
107. H. L. Handl, J. Vagner, H. I. Yamamura, V. J. Hruby, and R. J. Gillies (2004). Lanthanide-based time-resolved fluorescence of in cyto ligand–receptor interaction. *Anal. Biochem.* **330**, 242–250.
108. D. Somjen, F. Kohen, B. Gayer, T. Kulik, E. Knoll, and N. Stern (2004). Role of putative membrane receptors in the effect of androgens on human vascular cell growth. *J. Endocrin.* **180**, 97–106.
109. O. Zohar, M. Ikeda, H. Shinagawa, H. Inoue, H. Nakamura, D. Elbaum, D. L. Alkon, and T. Yoshioka (1998). Thermal imaging of receptor-activated heat production in single cells. *Biophys. J.* **74**, 82–89.
110. H. Frang, V. M. Mukkala, R. Syysto, P. Ollikka, P. Hurskainen, M. Scheinin, and I. Hemmila (2003). Nonradioactive GTP binding

assay to monitor activation of G protein-coupled receptor. *Assay. Drug Dev. Technol.* **1**, 275–280.
111. K. Xu, A. S. Stern, W. Levin, A. Chua, and L. T. Vassilev (2003). A generic time-resolved fluorescence assay for serine/threonine kinase activity: Application to Cdc7/Dbf4. *J. Biochem. Mol. Biol.* **36**, 421–425.
112. Y. Li, R. T. Cummings, B. R. Cunningham, Y. Chen, and G. Zhou (2003). Homogeneous assays for adenosine 5'-monophosphate-activated protein kinase. *Anal. Biochem.* **321**, 151–156.
113. J. A. Cruz-Aguado, Y. Chen, Z. Zhang, M. A. Brook, and J. D. Brennan (2004). Entrapment of Src protein tyrosine kinase in sugar-modified silica. *Anal. Chem.* **76**, 4182–4188.
114. T. M. Sadler, M. Achilleos, S. Ragunathan, A. Pitkin, J. LaRocque, J. Morin, R. Annable, L. M. Greenberger, P. Frost, and Y. Zhang (2004). Development and comparison of two nonradioactive kinase assays for I kappa B kinase. *Anal. Biochem.* **326**, 106–113.
115. L. Minor (2003). Receptor phosphorylation in a cell-based assay as a screen for receptor modulators. *Am. Pharm. Rev.* **6**, 96–98.
116. J. Hirata, C. F. de Jong, M. M. van Dongen, J. Buijs, F. Ariese, H. Irth, and C. Gooijer (2004). A flow injection kinase assay system based on time-resolved fluorescence resonance energy-transfer detection in the millisecond range. *Anal. Chem.* **76**, 4292–4298.
117. J. Whitfields, K. Harada, C. Bardelle, and J. M. Staddon (2003). High-throughput methods to detect dimerization of Bcl-2 family proteins. *Anal. Biochem.* **322**, 170–178.
118. K. Xu, C. Belunis, W. Chu, D. Weber, F. Podlaski, K. S. Huang, S. I. Reed, and L. T. Vassilev (2003). Protein–protein interactions involved in the recognition of p27 by E3 ubiquitin ligase. *Biochem. J.* **371**, 957–964.
119. V. Leblanc, V. Delaunay, L. J. Claude, F. Gas, G. Mathis, J. Grassi, and E. May (2002). Homogeneous time-resolved fluorescence assay for identifying p53 interactions with its protein partners, directly in a cellular extract. *Anal. Biochem.* **308**, 247–254.
120. D. Maurel, J. Kniazeff, G. Mathis, E. Trinquet, J. P. Pin, and H. Ansanay (2004). Cell surface detection of membrane protein interaction with homogeneous time-resolved fluorescence resonance energy transfer technology. *Anal. Biochem.* **329**, 253–262.
121. D. Ramsay, I. C. Carr, J. Pediani, J. F. Lopez-Gimenez, R. Thurlow, M. Fidock, and G. Milligan (2004). High-affinity interactions between human α_{1A}-adrenoceptor C-terminal splice variants produce homo- and heterodimers but do not generate the α_{1L} adrenoceptor. *Mol. Pharmacol.* **66**, 228–239.
122. L. Gazi, J. F. Lopez-Gimenez, M. P. Rudiger, and P. G. Strange (2003). Constitutive oligomerization of human D_2 dompamine receptors expressed in *Spodoptera frugiperda* 9 (Sf9) and in HEK293 cells. Analysis using co-immunoprecipitation and time-resolved fluorescence resonance energy transfer. *Eur. J. Biochem.* **270**, 3928–3938.
123. J. J. Carrillo, J. Pediani, and G. Milligan (2003). Dimers of class A G protein-coupled receptors function via agonist-mediated transactivation of associated G proteins. *J. Biol. Chem.* **278**, 42578–42587.
124. J. Liu, K. S. Knappenberger, H. Kack, G. Andersson, E. Nilsson, C. Dartsch, and C. W. Scott (2003). A homogeneous *in vitro* functional assay for estrogen receptors: Coactivator recruitment. *Mol. Endocrinol.* **17**, 346–355.
125. A. K. Galande, K. S. Bramlett, T. P. Burris, J. L. Wittliff, and A. F. Spatola (2004). Thioether side chain cyclization for helical peptide formation: Inhibitors of estrogen receptor–coactivator interactions. *J. Pept. Res.* **63**, 297–302.
126. A. L. Kung, S. D. Zabludoff, D. S. France, S. J. Freedman, E. A. Tanner, A. Vieira, S. Cornell-Kennon, J. Lee, B. Wang, J. Wang, K. Memmert, H. U. Naegeli, F. Petersen, M. J. Eck, K. W. Bair, A. W. Wood, and D. M. Livingston (2004). Small molecule blockade of transcriptional coactivation of the hypoxia-inducible factor pathway. *Cancer Cell* **6**, 33–43.
127. G. Allicotti, E. Borras, and C. Prinilla (2003). A time-resolved fluorescence immunoassay (DELFIA) increases the sensitivity of antigen-driven cytokine detection. *J. Immunoassay Immunochem.* **24**, 345–358.
128. H.-G. Zerves, J. C. Peter, M. Link, H. Gubler, and G. Scheel (2002). A multiparameter screening assay for assess the cytokine-induced expression of endothelial cell adhesion molecules. *Anal. Biochem.* **304**, 166–173.
129. K. Enomoto, Y. Aono, T. Mitsugi, K. Takahashi, R. Suzuki, M. Preaudat, G. Mathis, G. Kominami, and H. Takemoto (2000). High throughput screening for human interferon-γ production inhibitor using homogeneous time-resolved fluorescence. *J. Biomol. Screen.* **5**, 263–268.
130. E. Heyduk and T. Heyduk (1999). Architecture of a complex between the $\sigma 7$ subunit of *Escherichia coli* RNA polymerase and the nontemplate strand oligonucleotide. Luminescence resonance energy transfer study. *J. Biol. Chem.* **274**, 3315–3322.
131. V. Bergendahl, T. Heyduk, and R. R. Burgess (2003). Luminescence resonance energy transfer-based high-throughput screening assay for inhibitors of essential protein–protein interactions in bacterial RNA polymerase. *Appl. Environ. Microbiol.* **69**, 1492–1498.
132. V. Zhou, S. Han, A. Brinker, H. Klock, J. Caldwell, and X. J. Gu (2004). A time-resolved fluorescence resonance energy transfer-based HTS assay and a surface plasmon resonance-based binding assay for heat shock protein 90 inhibitors. *Anal. Biochem.* **331**, 349–357.
133. W. Aherne, A. Maloney, C. Prodromou, M. G. Rowlands, A. Hardcastle, K. Boxall, P. Clarke, M. I. Walton, L. Pearl, and P. Workman (2003). Assays for HSP90 and inhibitors. *Methods Mol. Med.* **85**, 149–161.
134. H. Butcher, W. Kennette, O. Collins, J. Demoor, and J. Koropatnick (2003). A sensitive time-resolved fluorescent immunoassay for metallothionein protein. *J. Immunol. Methods* **272**, 247–256.
135. S. E. Barrie, E. Eno-Amooquaye, A. Hardcastle, G. Platt, J. Richards, D. Bedford, P. Workman, W. Aherne, S. Mittnacht, and M. D. Garrett (2003). High-throughput screening for the identification of small-molecule inhibitors of retinoblastoma protein phosphorylation in cells. *Anal. Biochem.* **320**, 66–74.
136. S. M. Kopalakrishnan, J. Karvinen, J. L. Kofron, D. J. Burns, and U. Warrior (2002). Application of micro arrayed compound screening (μARCS) to identify inhibitors of caspase-3. *J. Biomo. Screen.* **7**, 317–323.
137. M. Preaudat, J. Ouled-Diaf, B. Alpha-Bazin, G. Mathis, T. Mitsugi, Y. Aono, K. Takahashi, and H. Takemoto (2002). A homogeneous capase-3 activity assay using HTRF technology. *J. Biomol. Screen.* **7**, 267–274.
138. H. Bazin, S. Guillemer, and G. Mathis (2002). Homogeneous phosphodiesterase and hybridization assays using europium cryptate:Oligonucleotide conjugates. *J. Fluoresc.* **12**, 245–248.
139. M. Gabourdes, V. Bourgine, G. Mathis, H. Bazin, and B. Alpha-Bazin (2004). A homogeneous time-resolved fluorescence detection of telomerase activity. *Anal. Biochem.* **333**, 105–113.
140. M. D. Boisclair, C. McClure, S. Josiah, S. Glass, S. Bottomley, S. Kamerkar, and I. Hemmilä (2000). Development of a ubiquitin transfer assay for high throughput screening by fluorescence resonance energy transfer. *J. Biomol. Screen.* **5**, 319–328.
141. N. Yabuki, S. Watanabe, T. Kudoh, S. Nihira, and C. Miyamato (1999). Application of homogeneous time-resolved fluorescence (HTRF^{TM}) to monitor poly-ubiquitination of wild-type p53. *Comb. Chem. High troughput. Screen.* **2**, 279–287.
142. A. C. Hamilton, J. Inglese, and M. Ferrer (2003). A PDZ domain-based assay for measuring HIV protease activity: Assay design considerations. *Protin. Sci.* **12**, 458–467.
143. A. Gharehbaghian, K. M. Haque, C. Truman, J. Newman, and B. A. Bradley (2002). Quantitation of natural killer cell precursors in man. *J. Immunol. Methods* **260**, 69–77.
144. K. Blomberg, R. Hautala, J. Lövgren, V. M. Mukkala, C. Lindqvist, and K. Akerman (1996). Time-resolved fluorometric assay for natural killer activity using targets cells labelled with a fluorescence enhancing ligand. *J. Immunol. Methods* **193**, 199–206.

145. D. Waddleton, C. Ramachandran, and Q. Wang (2002). Development of a time-resolved fluorescent assay for measuring tyrosine-phosphorylated proteins in cells. *Anal. Biochem.* **309**, 150–157.
146. D. Somjen, S. Katzburg, O. Sharon, A. M. Kaye, B. Gayer, F. Kohen, D. Hendel, and G. H. Posner (2004). Modulation of response to estrogen in cultured human female bone cells by a non-calcemic vitamin D analog: Changes in nuclear and membranal binding. *J. Steroid Biochem. Mol. Biol.* **89–90**, 393–395.
147. V. Marchi-Artzner, M. J. Brienne, T. Gulik-Krzywicki, J. C. Dedieu, and J. M. Lehn (2004). Selective complexation and transport of europium ions at the interface of vesicles. *Chemistry.* **10**, 2342–2350.
148. T. Chakrabasty, M. Xiao, R. Cooke, and P. R. Selvin (2002). Holding two heads together: Stability of the myosin II rod measured by resonance energy transfer between the heads. *Proc. Natl. Acad. Sci. U.S.A.* **99**, 6011–6016.
149. C. F. Becker, D. Clayton, G. Shapovalov, H. A. Lester, and G. G. Kochendoerfer (2004). On-resin assembly of a linkerless lanthanide(III)-based luminescence label and its application to the total synthesis of site-specifically labeled mechanosensitive channels. *Bioconjug. Chem.* **15**, 1118–1124.
150. M. E. Neville, K. W. Richau, L. T. Boni, L. E. Pflug, R. J. Robb, and M. C. Popescu (2000). A comparison of biodistribution of liposomal and soluble IL-2 by a new method based on time-resolved fluorometry of europium. *Cytokine* **12**, 1702–1711.
151. N. S. Ivey, E. N. Martin Jr, W. M. Scheld, and B. R. Nathan (2005). A new method for measuring blood–brain barrier permeability demonstrated with europium-bound albumin during experimental lipopolysaccharide (LPS) induced meningitis in the rat. *J. Neurosci. Methods* **142,** 91–95.
152. A. E. Soini, A. Kuusisto, N. J. Meltola, E. Soini, and L. Seveus (2003). A new technique for multiparametric imaging microscopy: Use of long decay time photoluminescent labels enables multiple color immunocytochemistry with low channel-to-channel crosstalk. *Microsc. Res. Technol.* **62**, 396–407.